

Stability of the rake during the 1992, Landers earthquake. An indication for a small stress release ?

Fabrice Cotton and Michel Campillo

LGIT (URA CNRS 733), Observatoire de Grenoble, Université Joseph Fourier, Grenoble, France

Abstract. We use the high quality data set of the Landers earthquake to study in detail the ability of strong motion inversions to resolve the rake during the rupture process. Initially, we constrain the rake to be constant on the fault. Several inversions with different rake values show that a pure strike slip gives the best fit to the data. In a second step, we have allowed the rake to vary spatially. Spatial rake variations are well resolved by the data and remain small; the data strongly constrain the earthquake to be a pure strike-slip event with almost no variation of the rake. We assume that the direction of the slip vector is always close to the direction of the applied stress, which itself is the vector sum of the pre-existing stress and the dynamic stress changes. The stability of the rake on a fault with a dynamical rupture process which is clearly heterogeneous suggests that the pre-existing stress level is quite homogeneous and that it dominates over the dynamic stress changes.

Introduction

In their study of the 1989 Loma Prieta earthquake several authors (Beroza [1991], Hartzell *et al.* [1991], Wald *et al.* [1991] and Steidl *et al.* [1991]) allow the rake to vary. All find strong variations in the slip direction over short distances (about 15 km). But the rake distributions in these studies are significantly different from one another and the question of the resolution of the rake in the case of Loma Prieta has been addressed by Beroza [1991] and by Cocco *et al.* [1994].

The 28 June 1992 Landers earthquake provides one of the most complete sets of near-source strong motion records. The good azimuthal distribution of strong motion instruments in the vicinity of the Landers event allows the characteristics of dynamic rupture propagation to be well resolved. Several studies (Cohee and Beroza, 1994; Wald and Heaton, 1994; Cotton and Campillo, 1995) have used these data to infer the detailed history of the rupture by waveform matching. The slip in all these models has been satisfactorily modeled with a constant rake of 180° . The difficult question is whether rake values are really constant and equal to 180° over the fault, or whether the data do not constrain these rake values so that other values of rake could equally well explain the strong motions. Using this unique set of records, we have concentrated our analysis on the rake variations: we find that this absence of rake variation is actually required by the data.

Copyright 1995 by the American Geophysical Union.

Paper number 95GL01773

0094-8534/95/95GL-01773\$03.00

Data and a priori parameterization

The strong motion station distribution is shown in Figure 1. Each of the 11 stations used in this study recorded three components of ground acceleration. The accelerograms are band-pass filtered between 20 s and 2.0 s, then doubly integrated in the frequency domain to obtain displacements.

The crustal model used in this study is that described in a forward modeling study of the Landers earthquake rupture by Campillo and Archuleta [1993], which was only slightly modified from Kanamori and Hadley [1975]. We assume that the surface offset and the aftershocks distribution give an image of the actual fault at depth. These observations lead us to consider a model which consists of three vertical distinct segments (30 km, 20 km, and 30 km long) oriented with different strikes (Figure 1).

Strong motion modeling and inversion procedure

The fault parameterization and modeling procedure is that of Cotton and Campillo [1995] except that we now allow the rake to vary by solving for both strike-slip and dip-slip components. We divide the fault plane into 48 subfaults. Each subfault is allowed to slip once. The ground motion v at a given station i and a given frequency ω can be represented as a linear sum of n subfault contributions:

$$v_i(\omega) = \sum_{k=1}^n (\Delta s_k u_k(\omega) + \Delta d_k u'_k(\omega)) \exp^{-i\omega t_k} S_k(R_k, \omega)$$

where u_k and u'_k represent the ground motion for a unit constant strike-slip (rake equal to 0°) and dip-slip (rake equal to 90°) on the subfault k . Δs_k , Δd_k , t_k , and S_k are the strike slip, the dip slip, the time delay, and the site response, respectively.

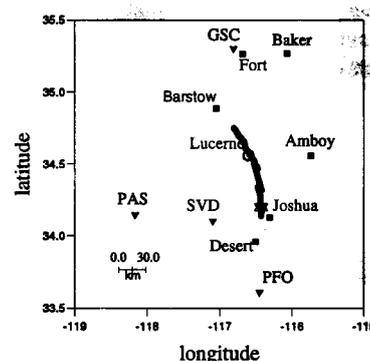


Figure 1. Location map displaying CDMG (squares), TERRAscope (triangles), and Southern California Edison (octagon) strong-motions stations used in this study. Heavy solid lines represent the surface rupture of the earthquake.

the beginning rupture time and the source function ($S(t)=0.5(1+\tanh(t+R/2,0)^2)$) of the k -th subfault depending on a single variable: the rise time R_k . In practice, each subfault is represented by an array of point sources separated by 500 meters. The point-source Green's functions are computed using a discrete wavenumber integration method associated with a reflection transmission matrix method.

The ground motion $v_i(\omega)$ can be considered as a function of the following parameters: $\Delta s_k, \Delta d_k, t_k$ and R_k . The elements of d consists of real and imaginary part of displacement spectra from all stations and all components (in the following d is represented by 3960 elements). The parameter vector p and data vector d are related by the function model vector f as $d=f(p)$. If we assume an initial parameter vector p_0 , we can iterate to the solution p_k by linearization of f around p_0 at the first iteration and around p_{k-1} at each subsequent iteration k . Using the observed data vector d_0 and an inversion algorithm based on *Tarantola and Valette* [1982], p_{k+1} is given by:

$$p_{k+1} = p_k + b(A_k^T C_d^{-1} A_k + C_p^{-1})^{-1} (A_k^T C_d^{-1} (d_0 - f(p_k)) + C_p^{-1} (p_0 - p_k))$$

Here A_k is the Jacobian matrix of $f(p_k)$, b is a damping constant between 0 and 1 used to prevent divergence, and C_p and C_d are the covariance matrices for p and d . We assume that off-diagonal elements of C_p and C_d are equal to 0. The diagonal elements of C_d and C_p are given by the data and parameter variances. In this inversion, we give a greater weight to the TERRAscope stations, which have an acquisition system with higher dynamic range by giving smaller variances ($C_d=0.25$) to these stations relative to the others ($C_d=1.0$). C_p is equal to 81.0 for all the parameters. These diagonal values were found after several test inversions to find the best convergence. The observed and synthetic amplitude spectra at each station are normalized by the maximum observed amplitude of the three components.

Results

As a first step, we have tried several inversions with constant rake on all the subfaults. In those inversions the ratio between the strike slip and the dip slip is held constant and the inversion gives only the rise time, the time of rupture and the slip amplitude (144 unknowns). The fit to the data is evaluated using the variance reduction between theoretical and observed seismograms as defined by *Cohee and Beroza* [1994]. A variance reduction of 100% means that the data are perfectly matched by our synthetics. Figure 2 gives the final variance reduction for each chosen value of rake. The rake which gives

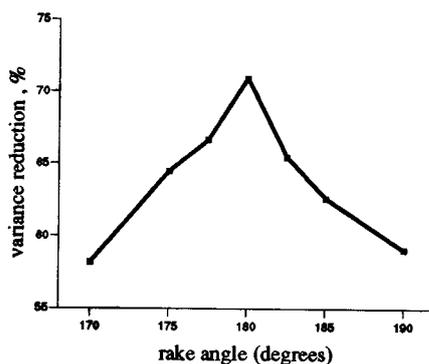


Figure 2. Variance reductions given by inversions performed with different rake directions. In those inversions the rake direction is the same on the all fault plane.

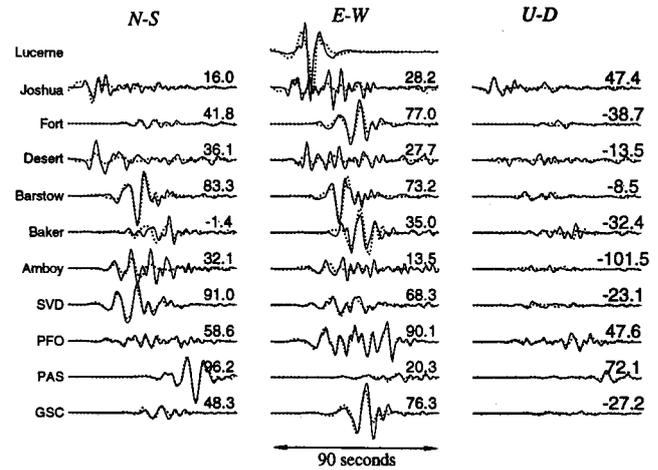


Figure 3. Strong motion seismograms of the Landers earthquake (solid line) compared with synthetic seismograms (dotted line). Each pair of data and theoretical seismograms is plotted at the same amplitude scale with the variance reduction shown to the right of each pair.

the best fit (variance reduction of 71%) is equal to 180° (pure strike slip). A variation in rake of 10° around this pure strike slip decreases the fit to the data significantly: with a rake of 190° and 170° the variance reduction are, respectively, 58% and 59%. These results also suggest that this type of study cannot be performed with only a visual evaluation of the fit. Indeed, models with a variance reduction of 58% give fits to the data which, visually, seem acceptable.

As a second step, the rake is allowed to vary spatially in the inversion (192 unknowns). The variance reduction between the data and synthetics with a starting model for the rake of 180° is 71.5%. Figure 3 shows the fit between data and synthetics. This value is very close to the variance reduction found in the inversion with constant rake of 180° , described above and presented in *Cotton and Campillo* [1995]. In other words, we do not improve the fit to the data by permitting the rake to vary during the procedure from an initial value of 180° . The difficult point is to know is whether spatial rake variations really are small or whether the inversion simply cannot determine these variations.

Since the inversion is not purely linear, the final values for the parameters which are not well constrained by the data are mostly dependent on the a priori value chosen in the starting model. If we choose different starting models, we identify the unresolved portion of the solution by the parameters which do not converge to a common value. We have performed our inversion procedure with 3 initial values of rake on the subfaults of the starting model p_0 : 170° , 180° and 190° . On each subfaults, the inversion procedure leads to final values of the rake which give a better fit to the data. For each a priori rake value chosen as a starting model, the numbers of subfaults with a given rake value in the final model are presented in an histogram Figure 4. Regardless of the initial values of the rake, most of the final values are between 175° and 185° . Even, if the initial a priori values of the rake is equal to 190° or 170° , the inversion changes these initial values to new values close to 180° . This shows that the final rake values do not depend on our a-priori choices. It is therefore clear from these tests that the data require the rupture to be almost pure strike-slip (when significant moment release occurred).

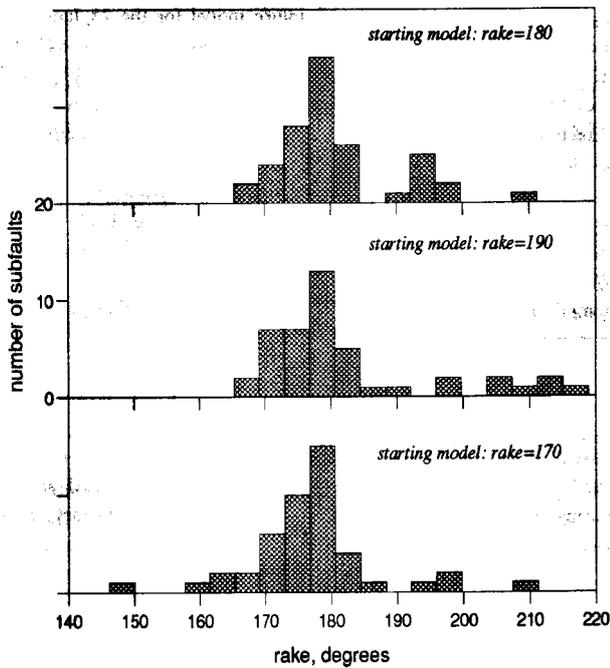


Figure 4. Distribution of the final rakes values found by our inversion with different a priori starting model (top: starting value of the rake equal to 170°, middle: 180°, bottom: 190°)

To illustrate this point, we have calculated for each subfault the mean and standard deviation of the rake values found by the inversions with three different starting models. Figure 5 shows for each subfault, the amplitude and direction of this mean slip vector of the west wall of the fault. Considering only the subfaults where the amplitude of slip is large (more than 1.5 m) we notice that most of the rakes are close to 180° (Figure 6). Most of the deviations of the rake with respect to 180° occur only on the Emerson and Camp Rock faults, farther than 40 km from the epicenter. One can also notice negative values of slip on the edge of the actual rupture zone. In spite of the lack of positivity constraints, these nonphysical negative values remains rare. This absence of positivity constraints allows to reduce the influence of the a priori choices on the final result of the inversion.

Discussion and conclusion

Nearly all the waveform inversion studies which have been done over the past 10 years to determine the slip histories of earthquakes have shown that the slip amplitudes, rupture velocities and rise times have a heterogeneous distribution on the fault plane. This is also the case for the Landers earthquake. Our results which prove the stability of the value of the rake, therefore seems surprising. How could the rake be spatially constant in a rupture process which has a very heterogeneous behavior ?

The total stress at a point on the fault plane is given by the frictional stress which is the result of an interaction between the pre-existing stress and the dynamic stress changes. If we assume that a highly heterogeneous rupture process results in spatial variability of dynamic stresses and that the sliding friction stress is collinear with the slip velocity, the stability of the rake on a fault which has a heterogeneous rupture process

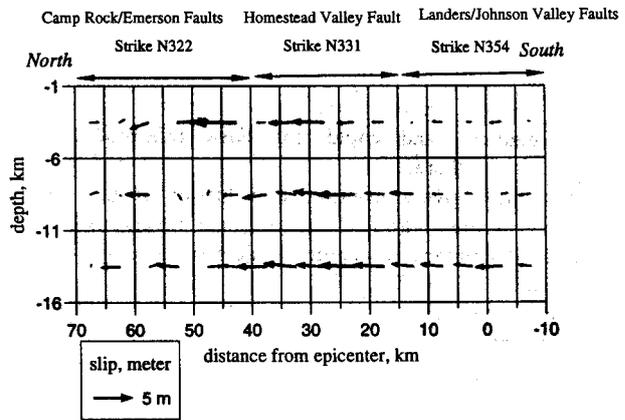


Figure 5. Vector plot of the rake as a function of position on all the subfaults.

leads to the 2 following propositions. 1): the spatial variations of the pre-existing stress are small and 2): this pre-existing stress probably dominates dynamic stress variations (partial stress release).

Hauksson [1994] used focal mechanisms of the background seismicity to determine the state of stress before 1992 in the Landers region. These data show that prior to the Landers earthquake spatial stress variations were small in agreement with our proposition 1). Hauksson [1994] also studied the aftershocks of the 1992 event and showed that the direction of the deviatoric stress tensor did not change significantly from the pre-event state in the southern and central part of the fault. This is where about 70% of the moment release occurred (Coehee and Beroza, 1994; Wald and Heaton, 1994; Cotton and Campillo, 1995), and is consistent with our proposition 2), at least for the southern part of the fault. According to Hauksson [1994], since the strike of the rupture changes as it propagates to the north, the angle between the maximum principal stress and the orientation of fault ranged from 37° (near the epicenter) to 58° (in the north). This means that the ratio between the dynamic shear stress release and the preexisting shear stress becomes greater as the rupture propagates to the north which could explain the greater variability of rake found on the Camp Rock and Emerson faults. Hauksson [1994] also found a greater variability of the aftershocks in the northern section, and interpreted this to mean that much of the uniform component of the shear stress had been removed on the Emerson and Camp Rock faults. However, all the inversions performed with the data of the Landers earthquake (Coehee and Beroza, 1994; Wald

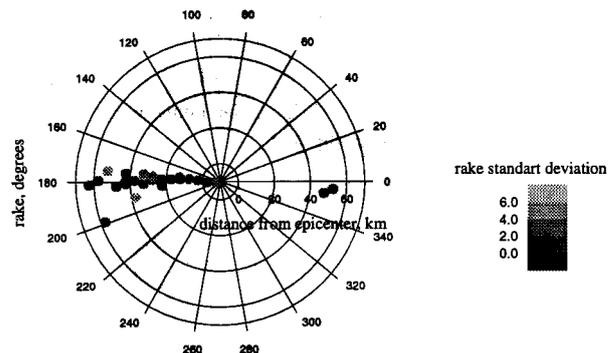


Figure 6. Rake values function of the distance from the epicenter when significant slip (>1.5m) was found.

and Heaton 1994; Cotton and Campillo, 1995) have shown for this section of the fault, although the slip was very high (>5m), it was located only near the surface. Therefore coseismic slip effect did not involve the entire brittle crust in the northern segment, and could not have relieved all the preexisting stress there.

It is difficult to give a quantitative evaluation of the ratio of initial stress to stress drop. Comparing our inversion results with published spontaneous rupture models is not easy because all of these models have been run for high ratio of initial stress to stress drop or under the assumption of a constant rake. For example, in Das [1981] the ratio of initial stress to stress drop is 5. These values can be considered as upper bounds of the values required to ensure a rupture with a constant rake, assuming an homogeneous initial stress. The development of 3D dynamic codes of spontaneous rupture in stratified media is needed to study quantitatively the variability of dynamic stresses and rake in heterogeneous rupture processes. An original approach is proposed by Spudich [1992] who discusses the conditions under which it is possible to determine the absolute stress level at a point on a fault from observation of temporal rake rotations at that point. He shows that if the rake rotates, there is a unique absolute stress consistent with this motion. We cannot use these results because the inversion of temporal rake variations strongly increases the number of parameters and therefore the rake at one point of the fault is constrained to be constant in our inversion.

Finally, how can we explain the strong rake variations found for the Loma Prieta earthquake but small variations for the Landers earthquake? One possible explanation is a bias in the rake estimates due to a lack of resolution in the data set of the Loma Prieta earthquake (Beroza [1991]). In fact, Cocco *et al.* [1994] has shown that strong motion inversions are able to find many physically acceptable models which fit these data equally well. The partition between the constrained and unconstrained parts of the solution depends on the distributions of stations, fault geometry and mechanism. It must be analysed for each particular case. A second possible explanation of the contrast of amplitude of rake variations between the Loma Prieta and Landers earthquakes may be due to the near total stress drop and near-frictionless heterogeneous faulting during the 1989 Loma Prieta, California, earthquake as suggested by Zoback and Beroza [1993] who analysed the variation of focal mechanism of aftershocks. On the contrary, Landers earthquake released only partially the stress on the Johnson Valley and Homestead Valley faults.

Acknowledgments. We thank S. Das and M. Cocco for stimulating conversations. Comments by J. Barker and two anonymous reviewers are greatly acknowledged.

References

Beroza, G.C., Near-source modeling of the Loma Prieta earthquake: Evidence for heterogeneous slip and implications for the earthquake hazards, *Bull. Seismol. Soc. Am.*, 81, 1603-1621, 1991.

- Campillo, M. and R.J. Archuleta, A rupture model for the 28 June 1992 Landers, California Earthquake, *Geophys. Res. Lett.*, 20, 647-650, 1993.
- Cocco, M., M.G. Guatteri and H. Hunstad, On the variation of slip direction during earthquake rupture: supporting and conflicting evidence from the 1989 Loma Prieta earthquake., AGU Fall Meeting, San Francisco, December 5-9, 1994.
- Cohee, B.P. and G.C. Beroza, Slip distribution of the 1992 Landers earthquake and its implications for earthquake source mechanism, *Bull. Seismol. Soc. Am.*, 84, 692-712, 1994.
- Cotton, F. and M. Campillo, Frequency domain inversion of strong motions: application to the 1992 Landers earthquake., *J. Geophys. Res.*, 100, 3961-3975, 1995.
- Das, S., Three-dimensional spontaneous rupture propagation and implications for the earthquake source mechanism., *Geophys. J.R. Astron. Soc.*, 67, 375-393, 1981.
- Hartzell, S.H., G.S. Steward and C. Mendoza, Comparison of L1 and L2 norms in a teleseismic waveform inversion for the slip history of the Loma Prieta, California, earthquake, *Bull. Seismol. Soc. Am.*, 81, 1518-1539, 1991.
- Hauksson, E., State of stress from local mechanism before and after the 1992 Landers earthquake sequence, *Bull. Seismol. Soc. Am.*, 84, 917-934, 1994.
- Kanamori, H. and D. Hadley, Crustal structure and temporal velocity change in southern California, *Pure Appl. Geophys.*, 113, 257-280, 1975.
- Spudich, P.K.P., On the inference of absolute stress levels from seismic radiation, *Tectonophysics*, 211, 99-106, 1992.
- Steidl, J.H., R.J. Archuleta and S.H. Hartzell, Rupture history of the 1989 Loma Prieta, California, earthquake, *Bull. Seismol. Soc. Am.*, 81, 1573-1602, 1991.
- Tarantola, A. and B. Valette, Generalized nonlinear inverse problem solved using the least squares criterion, *Rev. Geophys. Space Phys.*, 20, 219-232, 1982.
- Wald, D.J., D.V. Helmberger and T.H. Heaton, Rupture model of the 1989 Loma Prieta earthquake from the inversion of strong-motion and broadband teleseismic data, *Bull. Seismol. Soc. Am.*, 81, 1540-1572, 1991.
- Wald, D.J. and T.H. Heaton, Spatial and temporal distribution of slip for the 1992 Landers, California, earthquake., *Bull. Seismol. Soc. Am.*, 3, 668-691, 1994.
- Zoback, M.D. and G.C. Beroza, Evidence for near-frictionless faulting in the 1989 (M 6.9) Loma Prieta, California, earthquake and its aftershocks, *Geology*, 21, 181-185, 1993.

F. Cotton, IRIGM-LGIT BP 53 X 38041 Grenoble Cedex, France.
(email: cotton@lgit.observ-gr.fr)
M. Campillo, IRIGM-LGIT BP 53 X 38041 Grenoble Cedex,
France. (email: campillo@lgit.observ-gr.fr)

(Received April 13, 1995; accepted June 6, 1995)